Emergent Gravitation, Spacetime Geometry, and Relativistic Quantum Dynamics from a Bounded Vacuum

Tanuj Kumar[1,*], Vandana[1], Jyoti[2]

[1]Department of Physics and Astronomical Sciences, Central University of Jammu, Rahya-Suchani, Bagla, Jammu, India-181143

[2]Department of Physics, Government College for Women, Gurawara, Rewari, Haryana, India-123035

***Corresponding author:** tanuj.phy@cujammu.ac.in

Date: 20-August-2026

Abstract

We develop an effective continuum framework in which the physical vacuum is characterized by a bounded scalar capacity field $\Phi(\boldsymbol{x}, t)$, with normalized remaining-capacity fraction $f = \Phi/c^2$. Matter is represented by localized depletion of this capacity, while gravitation arises from the associated redistribution of the remaining vacuum response. In the weak-field limit, the governing equation reduces to the Poisson equation and reproduces Newtonian gravity. A nonlinear capacity-dependent response yields the exterior solution $f(r) = \sqrt{1 - 2Gm/(rc^2)}$. Relating the local capacity fraction to temporal and reciprocal radial scaling reconstructs the Schwarzschild exterior line element $ds^2 = -f^2c^2dt^2 + f^{-2}dr^2 + r^2d\Omega^2$, together with its standard weak-field gravitational optical response. The same continuum dynamics admit localized intrinsic oscillations which, under the quantum normalization $\hbar\omega_0 = mc^2$, yield the Planck–Einstein and de Broglie relations through Lorentz transformation of the intrinsic phase. The resulting dispersion relation takes the Klein–Gordon form and reduces to the Schrödinger equation in the nonrelativistic limit. Massive excitations propagate subluminally, whereas massless disturbances remain nondispersive with limiting propagation speed c. The framework thus provides a common continuum description of vacuum depletion, emergent gravitation and spacetime scaling, and relativistic matter-wave dynamics, while identifying strong-field dynamical phenomena as a potential regime for distinguishing predictions.

Keywords: Bounded vacuum; Emergent gravitation; Vacuum-capacity field; Matter waves; Klein-Gordon equation; Unified continuum theory.

I. Introduction

General relativity (GR) and quantum mechanics constitute the two principal foundations of modern physics. GR describes gravitation through spacetime geometry and has been extensively confirmed from Solar-System scales to gravitational-wave observations [1-4], while quantum mechanics and quantum field theory provide the framework for microscopic matter and the nongravitational interactions of the Standard Model [5-7]. Despite their empirical success, the two theories are founded on conceptually different descriptions, and establishing a consistent connection between gravitation and quantum physics remains a central problem in fundamental physics.

Several approaches address this problem from different perspectives, including string theory, loop quantum gravity, causal dynamical triangulations, and asymptotic safety [8-11]. A complementary direction is provided by emergent-gravity ideas, in which spacetime or gravitational dynamics arise from more fundamental microscopic degrees of freedom. Sakharov related gravity to quantum-vacuum fluctuations, Jacobson connected Einstein's equation with thermodynamic relations, and related emergent approaches have explored gravity as a collective or statistical phenomenon [12-14]. These developments motivate consideration of the physical vacuum as more than a passive background.

The quantum vacuum itself exhibits observable physical effects. Zero-point fluctuations, vacuum polarization, the Casimir effect, and the Lamb shift demonstrate that the vacuum possesses nontrivial dynamical properties [15, 16]. An apparently separate clue arises from the wave description of matter. De Broglie associated a massive particle with an intrinsic periodicity whose rest-frame angular frequency is determined by its rest energy[17-19],

$$\omega_0 = \frac{mc^2}{\hbar} \tag{1.1}$$

Through phase harmony, this intrinsic periodicity is related to the relativistic matter-wave phase and ultimately to the de Broglie wavelength. The connection between rest energy, proper time, and quantum phase has also received renewed attention in atom-interferometric studies, although the interpretation of such experiments as direct measurements of a Compton-frequency clock remains debated [20-23].

Motivated by these observations, we investigate an effective continuum description in which the vacuum is characterized by a bounded scalar capacity field $\Phi(\boldsymbol{x}, t)$, with equilibrium value $\Phi_0 = c^2$. The central hypothesis is that matter corresponds to localized depletion of this capacity, while gravitation arises from the associated redistribution of the remaining vacuum response. Rather than assuming spacetime geometry as the starting point, temporal and spatial scaling are related to the local normalized capacity $f = \Phi/c^2$. The nonlinear exterior solution is shown to generate the Schwarzschild metric, with the corresponding effective optical response reproducing the standard gravitational light deflection. The same continuum supports localized intrinsic oscillations which, after the quantum normalization $\hbar\omega_0 = mc^2$, generate the relativistic matter-wave phase, Klein–Gordon structure, and Schrödinger nonrelativistic limit.

The aim is therefore not to replace established GR or quantum theory by assumption, but to examine whether several of their characteristic structures can arise as different limits of a single bounded-vacuum continuum. Section II introduces the vacuum-capacity field and its relativistic normalization. Section III develops matter loading and gravitational redistribution, while Sec. IV formulates the continuum dynamics through an effective action. Section V extends the response to the nonlinear strong-field regime, and Sec. VI derives the emergent Schwarzschild geometry and its optical consequences. Sections VII and VIII develop relativistic matter-wave dynamics and the nonrelativistic and localization limits, respectively, while Sec. IX considers a spatially varying capacity background. Physical consequences and possible distinguishing predictions are discussed in Sec. X, limitations in Sec. XI, and the principal results are summarized in Sec. XII.

II. Vacuum-Capacity Field: Physical Foundations and Relativistic Normalization

The present framework is founded on the hypothesis that the physical vacuum can be described as a continuous medium characterized by a scalar vacuum-capacity field $\Phi(\boldsymbol{x}, t)$. Unlike the Newtonian gravitational potential, which is conventionally introduced as a field sourced by a prescribed matter distribution, Φ is taken as the primary continuum variable specifying the local state of the vacuum. Matter, gravitation, and the effective spacetime geometry are subsequently interpreted as manifestations of localized depletion and redistribution of this underlying field.

The absolute scale of Φ is fixed by relativistic energy normalization. For a particle of inertial mass m, special relativity gives the rest energy $E_0 = mc^2$ [24]; division by m identifies c^2 as the universal relativistic energy scale per unit mass. We therefore assign the homogeneous undeformed vacuum the equilibrium capacity

$$\Phi_0 = c^2 \tag{2.1}$$

The field Φ consequently has dimensions of specific energy, identical to those of the Newtonian gravitational potential, but with an absolute reference scale fixed by relativistic normalization. Its connection with conventional gravitation follows from the weak-field limit of general relativity. For the Newtonian potential ϕ_N, with $|\phi_N|/c^2 \ll 1$, one has $g_{00} \simeq -(1 + 2\phi_N/c^2)$, while the specific energy of a slowly moving test particle approaches $c^2 + \phi_N$ [4, 25, 26]. This motivates the weak-field correspondence

$$\Phi \simeq c^2 + \phi_N \tag{2.2}$$

For a conventional static spherical source of mass M,

$$\phi_N(r) = -\frac{GM}{r}, \tag{2.3}$$

so that the conventional weak-field expression becomes $\Phi \simeq c^2 - GM/r$. In the present framework, however, Φ is the primary continuum field, whereas $\phi_N = \Phi - c^2$ represents only its weak-field departure from equilibrium. We therefore introduce a continuum parameter m characterizing the integrated strength of a localized, self-consistent vacuum deformation. Its weak-field exterior profile is written

$$\Phi(r) \simeq c^2 - \frac{Gm}{r} \tag{2.4}$$

At this stage, m is not assumed *a priori* to represent material, inertial, or gravitational mass; its physical identification follows in Sec. III from global vacuum redistribution and Newtonian correspondence. Equation (2.4) is likewise not a fundamental definition of Φ, but the weak-field exterior realization of a localized continuum deformation.

This behavior naturally motivates characterizing the deformation by the reduction of the local capacity relative to equilibrium. We therefore define the vacuum-capacity deficit by

$$\Delta\Phi \equiv c^2 - \Phi, \qquad \Delta\Phi(r) \simeq \frac{Gm}{r}, \tag{2.5}$$

and introduce the normalized remaining-capacity fraction

$$f \equiv \frac{\Phi}{c^2}, \tag{2.6}$$

together with the normalized depletion fraction

$$d \equiv \frac{\Delta\Phi}{c^2} = 1 - f \tag{2.7}$$

Here f and d are complementary dimensionless measures of the same local continuum state: f specifies the fraction of vacuum capacity remaining, whereas d specifies the fraction depleted relative to equilibrium. Since Φ represents the remaining physical capacity, the equilibrium value c^2 defines the maximum available capacity, while complete local depletion corresponds to vanishing remaining capacity. The physical domain is therefore

$$0 \le \Phi(\boldsymbol{x}, t) \le c^2, \qquad 0 \le f \le 1, \qquad 0 \le d \le 1 \tag{2.8}$$

Thus, the homogeneous undeformed vacuum corresponds to $\Phi = c^2$, $f = 1$, and $d = 0$, whereas the limiting completely depleted state corresponds to $\Phi = 0$, $f = 0$, and $d = 1$. For the weak-field spherical configuration of Eq. (2.4),

$$f(r) \simeq 1 - \frac{Gm}{rc^2}, \qquad d(r) \simeq \frac{Gm}{rc^2} \tag{2.9}$$

Accordingly, $Gm/(rc^2)$ measures the leading fractional depletion associated with a localized self-consistent vacuum deformation. In the weak-field regime $d \ll 1$ and $f \simeq 1$, whereas finite depletion probes the bounded capacity of the continuum and requires the self-consistent constitutive response developed in Sec. III.

The present section therefore establishes only the fundamental field variable, its normalization, its correspondence with the conventional weak-field potential, and its bounded physical domain. No nonlinear constitutive law is imposed at this stage. This separation is important: the bound $0 \le \Phi \le c^2$ specifies the admissible continuum state, whereas the manner in which the available response changes with depletion is determined subsequently from the continuum dynamics. The resulting bounded scalar structure provides the foundation for vacuum redistribution, emergent gravitation, and the finite-depletion dynamics developed in the following sections.

III. Matter, Vacuum Redistribution and Emergent Gravitation

A. Self-Consistent Vacuum Redistribution and the Governing Field Equation

The vacuum-capacity field Φ introduced in Sec. II is regarded as the fundamental scalar variable describing the local state of the bounded vacuum continuum. Matter is represented as a localized reduction of the equilibrium capacity $\Phi_0 = c^2$, rather than as an externally prescribed fundamental source, and gravitation is consequently interpreted as the equilibrium redistribution of the surrounding vacuum capacity. At the continuum level, a localized configuration is characterized by a coarse-grained vacuum-loading density $\rho_{\text{load}}(\boldsymbol{x})$, with total integrated loading

$$m = \int_V \rho_{\text{load}}(\boldsymbol{x})\, d^3x \tag{3.1}$$

At this stage, m is introduced only as an integrated continuum parameter and is not assumed a priori to represent inertial or gravitational mass; its physical identification follows from the weak-field correspondence below. To describe the redistribution locally, we introduce the vacuum-capacity flux $\boldsymbol{J}_\Phi$ [27, 28]. In static equilibrium, a localized loading acts as a sink of the surrounding redistribution, giving the local balance relation

$$\nabla \cdot \boldsymbol{J}_\Phi = -\alpha \rho_{\text{load}}, \tag{3.2}$$

where α fixes the normalization between localized loading and vacuum-capacity flux. In the weak-field regime, $\Phi = c^2 + \delta\Phi$, with $|\delta\Phi| \ll c^2$, and the undepleted vacuum is homogeneous and isotropic. The leading spatial response is therefore governed by the capacity gradient. Denoting the reference response coefficient of the undepleted continuum by T_0, the corresponding linear flux is

$$\boldsymbol{J}_\Phi = -T_0 \nabla\Phi \tag{3.3}$$

The coefficient T_0 is not introduced here as an additional gravitational coupling. It is the reference coefficient multiplying the spatial gradient-energy term in the continuum action developed in Sec. IV and Sec. V; Eq. (3.3) is its corresponding static linear flux. Since T_0 is constant in the undepleted weak-field regime, only its ratio with the normalization in Eq. (3.2) enters the static field equation. Substitution gives

$$\nabla^2\Phi = \frac{\alpha}{T_0}\rho_{\text{load}} \tag{3.4}$$

Equation (3.4) is therefore the leading linear, local, and isotropic realization of the static vacuum-redistribution balance about $\Phi = c^2$. Outside the localized configuration, $\rho_{\text{load}} = 0$, so $\nabla^2\Phi = 0$. For a static spherically symmetric configuration, $\Phi = \Phi(r)$, this becomes $r^{-2} d[r^2(d\Phi/dr)]/dr = 0$. Integrating twice and imposing the equilibrium boundary condition $\Phi(r \to \infty) = c^2$ gives

$$\Phi(r) = c^2 - \frac{C_1}{r} \tag{3.5}$$

Thus, the inverse-radius dependence follows from the static balance equation, spherical symmetry, and the asymptotic boundary condition rather than being independently imposed. The integration constant is fixed by the weak-field correspondence of Sec. II, $\Phi - c^2 \simeq \phi_N$. Since the Newtonian exterior potential of an isolated spherical configuration is $\phi_N = -Gm/r$ [4, 29, 30], comparison with Eq. (3.5) gives $C_1 = Gm$. Integrating Eq. (3.4) over a volume enclosing the complete configuration and applying Gauss's theorem gives $(\alpha/T_0)m = \oint \nabla\Phi \cdot d\boldsymbol{S} = 4\pi Gm$, and hence $\alpha/T_0 = 4\pi G$. The normalized weak-field equation and exterior solution are therefore

$$\boxed{\nabla^2\Phi = 4\pi G\rho_{\text{load}}, \qquad \Phi(r) = c^2 - \frac{Gm}{r}.} \tag{3.6}$$

Equivalently, Eqs. (3.2) and (3.3) give the flux balance $\nabla \cdot \boldsymbol{J}_\Phi = -4\pi G T_0 \rho_{\text{load}}$. Thus, T_0 sets the continuum response scale but cancels from the normalized static gravitational equation.

The continuum parameter m introduced in Eq. (3.1) is thereby identified operationally with gravitational mass in the weak-field limit rather than assigned this meaning from the outset. Correspondingly, $\Phi - c^2 = -Gm/r = \phi_N$, so the Newtonian potential appears as the weak-field departure of the vacuum-capacity field from equilibrium. For a weakly coupled test body of inertial mass m_t, the gravitational energy shift $E_{\text{grav}} = m_t(\Phi - c^2)$ gives $\boldsymbol{F} = -m_t\nabla\Phi$, and hence

$$\boldsymbol{a} = -\nabla\Phi = -\frac{Gm}{r^2}\hat{\boldsymbol{r}} \tag{3.7}$$

The cancellation of m_t gives the universality of weak-field free fall. The physical picture is illustrated schematically in Fig. 1: the homogeneous vacuum corresponds to $\Phi = c^2$, whereas a localized configuration is represented by a smooth depletion $\Delta\Phi > 0$. The surrounding vacuum capacity redistributes toward its asymptotic equilibrium value, producing the gradient $\nabla\Phi$ and the acceleration $\boldsymbol{a} = -\nabla\Phi$.

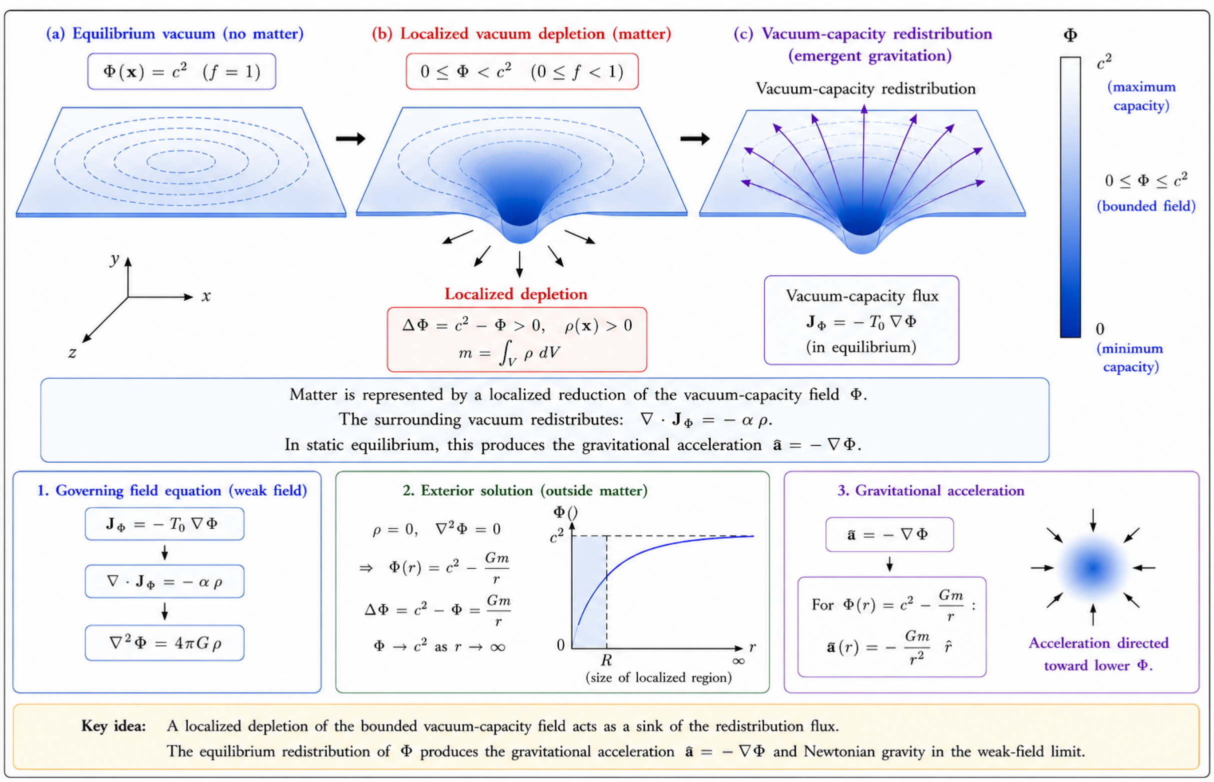

Figure 1. Localized vacuum-capacity depletion and the resulting gravitational redistribution.

The linear description is valid only for small departures from equilibrium, $|\Phi - c^2| \ll c^2$, for which the transmission coefficient may be approximated by its reference value T_0. At finite depletion, the available continuum response becomes dependent on the local vacuum state. The relation between localized loading and the finite capacity of the vacuum is established globally in Sec. III.B, while the resulting nonlinear redistribution equation and strong-field solution are developed in Sec. V.

B. Global Vacuum Redistribution, Mass, and Bounded Localization

The local field equation obtained in Sec. III.A also provides a global characterization of a localized vacuum deformation. Integrating $\nabla^2\Phi = 4\pi G\rho_{\text{load}}$ over a volume V enclosing the complete configuration and applying Gauss's divergence theorem [28, 31, 32] gives

$$m = \frac{1}{4\pi G}\oint_{\partial V} \nabla\Phi \cdot d\boldsymbol{S} \tag{3.8}$$

Thus, the integrated loading $m = \int_V \rho_{\text{load}}\, d^3x$ is determined by the total flux of the vacuum-capacity gradient through any closed surface surrounding the configuration. For spherical symmetry, Eq. (3.8) gives $r^2 d\Phi/dr = Gm$, which, together with $\Phi \to c^2$ as $r \to \infty$, reproduces $\Phi = c^2 - Gm/r$. The parameter m is therefore identified globally with gravitational mass through the asymptotic redistribution of the vacuum-capacity field.

The bounded condition $0 \le \Phi \le c^2$ established in Sec. II places a direct restriction on the linear exterior solution. From $\Phi = c^2 - Gm/r \ge 0$, one obtains

$$r \ge L_c \equiv \frac{Gm}{c^2} \tag{3.9}$$

The scale L_c is the radius at which an extrapolation of the linear solution would exhaust the available vacuum capacity. It therefore characterizes the breakdown scale of the linear approximation rather than an exact strong-field boundary or the physical radius of the localized configuration. For a configuration characterized by a length L, the same boundedness condition gives $m/L \le c^2/G$, naturally identifying the characteristic undepleted vacuum-capacity scale

$$\mu_0 \equiv \frac{c^2}{G} \tag{3.10}$$

The relation between localized loading and the bounded capacity follows directly from the weak-field profile. At the characteristic scale L, $\Delta\Phi = Gm/L$; using $1 - f = \Delta\Phi/c^2$ therefore gives

$$\lambda \equiv \frac{m}{L} = \mu_0(1 - f) \tag{3.11}$$

Thus, λ measures the portion of the finite vacuum capacity associated with localized depletion. In the homogeneous state $f = 1$, the loading vanishes, whereas the extrapolated depletion limit $f \to 0$ corresponds to $\lambda \to \mu_0$. Since the depleted and remaining fractions are complementary, $1 = (1 - f) + f$, the total capacity may equivalently be partitioned as $\mu_0 = \lambda + \mu$, giving

$$\mu = \mu_0 f \tag{3.12}$$

Equation (3.12) is therefore not introduced as an independent constitutive relation: it follows directly from the bounded-capacity partition together with Eq. (3.11). Here λ characterizes the portion associated with localized depletion, while μ represents the capacity remaining available for continuum response.

A corresponding characteristic elastic tension is defined as the localized energy per unit localization length, since in an elastic continuum the energy required per unit extension has the dimensions of force (tension). Thus, using $E \sim mc^2$ and the limiting localization length $L_c = Gm/c^2$, one obtains

$$T_0 \equiv \frac{mc^2}{L_c} = \frac{c^4}{G} = \mu_0 c^2 \tag{3.13}$$

The scale c^4/G is closely related to the maximum-force or maximum-tension scale discussed in general relativity [33-35]. In the present framework, however, T_0 follows from the relativistic energy normalization and the localization scale imposed by bounded vacuum capacity. It therefore provides the reference response scale of the undepleted continuum and is the same coefficient entering the linear gradient response of Sec. III.A and the continuum action developed in Sec. IV.

The propagation speed of a continuum excitation is determined by the ratio of its elastic and inertial response coefficients, $v^2 = T/\mu$ [28, 32]. For the homogeneous vacuum, relativistic normalization requires $v = c$, and Eq. (3.13) indeed gives $T_0/\mu_0 = c^2$. Requiring the same invariant propagation scale for the locally remaining continuum gives $T/\mu = c^2$. Since Eq. (3.12) already gives $\mu = \mu_0 f$, the corresponding local response follows as

$$T = \mu c^2 = T_0 f \tag{3.14}$$

Consequently,

$$\frac{T}{\mu} = \frac{T_0}{\mu_0} = c^2 \tag{3.15}$$

Thus, finite depletion reduces the available inertial and elastic responses by the same remaining-capacity fraction f, while their ratio remains fixed. The characteristic propagation speed of the continuum therefore remains c. Importantly, $T = T_0 f$ is not introduced as an independent constitutive prescription: once the remaining capacity $\mu = \mu_0 f$ is obtained from the bounded-capacity partition, it follows from the invariant propagation condition $T/\mu = c^2$.

The resulting hierarchy is therefore $L_c = Gm/c^2$ for the characteristic onset of significant depletion, $\mu_0 = c^2/G$ and $T_0 = c^4/G$ for the undepleted capacity and elastic-response scales, and $\mu = \mu_0 f$ and $T = T_0 f$ for the locally available responses. These relations provide the continuum parameters required by the action formulation of Sec. IV and the finite-capacity redistribution developed subsequently.

IV. Action Principle and Unified Continuum Dynamics

A. Effective Action Principle and Unified Continuum Dynamics

The static analysis of Sec. III establishes the characteristic vacuum-capacity and elastic-response scales $\mu_0 = c^2/G$ and $T_0 = c^4/G$. It also shows that finite depletion reduces the locally available response according to $\mu = \mu_0 f$ and $T = T_0 f$. To formulate the dynamics systematically, the bounded-vacuum continuum is described by Hamilton's principle, which provides a standard variational basis for continuum and field dynamics [28, 32, 36].

The dynamical variable is chosen to be the local vacuum-capacity deficit

$$\varphi(\boldsymbol{x},t) \equiv c^2 - \Phi(\boldsymbol{x},t), \tag{4.1}$$

where $0 \leq \varphi \leq c^2$. The homogeneous vacuum corresponds to $\varphi = 0$, while finite φ represents a local departure from equilibrium.

The effective action is written as

$$S = \int dt\, d^3x\, \mathcal{L}, \tag{4.2}$$

with the local continuum Lagrangian density

$$\mathcal{L} = \frac{1}{2}\mu(\partial_t\varphi)^2 - \frac{1}{2}T \mid \nabla\varphi \mid^2 - U(\varphi) + J\varphi. \tag{4.3}$$

The first term represents the inertial contribution associated with temporal variations of the vacuum deficit, the second represents the elastic energy associated with spatial redistribution, $U(\varphi)$ describes the local restoring response, and J represents coarse-grained external loading. Quadratic kinetic and deformation-energy terms constitute the standard lowest-order structure of linear continuum actions [28, 32, 36].

For prescribed continuum coefficients, application of Hamilton's principle, $\delta S = 0$ and using $\frac{\partial \mathcal{L}}{\partial \varphi} - \partial_t\left(\frac{\partial \mathcal{L}}{\partial(\partial_t\varphi)}\right) - \nabla \cdot \left(\frac{\partial \mathcal{L}}{\partial(\nabla\varphi)}\right) = 0$, gives the field equation in the useful flux-divergence form

$$\boxed{\mu\frac{\partial^2\varphi}{\partial t^2} - \nabla \cdot (T\nabla\varphi) + \frac{dU}{d\varphi} = J.} \tag{4.4}$$

The spatial contribution is therefore governed by the divergence of the elastic-response flux $T\nabla\varphi$, rather than by $T\nabla^2\varphi$ in general.

In the linear regime, $f \simeq 1$, and the continuum coefficients may therefore be approximated by their equilibrium values μ_0 and T_0. Here μ_0 and T_0 should be understood as the appropriately normalized coefficients entering the continuum Lagrangian density. Their ratio is fixed by the characteristic capacity scales established in Sec. III.B, $\frac{T_0}{\mu_0} = c^2$. This distinction allows the three-dimensional action to retain the required density normalization while preserving the physical ratio obtained from the bounded-capacity argument.

Applying Hamilton's principle, $\delta S = 0$, gives the Euler–Lagrange equation

$$\mu_0\frac{\partial^2\varphi}{\partial t^2} - T_0\nabla^2\varphi + \frac{dU}{d\varphi} = J \tag{4.5}$$

Using $\mu_0 = T_0/c^2$, Eq. (4.5) may equivalently be written in terms of T_0 as

$$\frac{T_0}{c^2}\frac{\partial^2\varphi}{\partial t^2} - T_0\nabla^2\varphi + \frac{dU}{d\varphi} = J \tag{4.6}$$

Thus, the characteristic propagation scale c enters through the ratio of the inertial and elastic responses rather than as an independently introduced wave velocity.

For small departures from equilibrium, the restoring potential may be expanded about its stable minimum as

$$U(\varphi) = U_0 + \frac{1}{2}\mu_0\omega_0^2\varphi^2 + O(\varphi^3), \tag{4.7}$$

where U_0 has no effect on the field equation and ω_0 characterizes the intrinsic small-amplitude oscillation. Since the physical field is bounded over $0 \le \varphi \le c^2$, higher-order terms may describe the nonlinear restoring response at finite depletion.

In the linear regime, $dU/d\varphi \simeq \mu_0\omega_0^2\varphi$, and Eq. (4.5) becomes

$$\frac{T_0}{c^2}\frac{\partial^2\varphi}{\partial t^2} - T_0\nabla^2\varphi + \frac{T_0\omega_0^2}{c^2}\varphi = J \tag{4.8}$$

Dividing by T_0 gives the normalized master equation

$$\frac{1}{c^2}\frac{\partial^2\varphi}{\partial t^2} - \nabla^2\varphi + \frac{\omega_0^2}{c^2}\varphi = \frac{J}{T_0} \tag{4.9}$$

Equation (4.9) is the linear dynamical equation governing propagation and intrinsic oscillation of vacuum-capacity disturbances. Although its mathematical structure is Klein–Gordon-like, no quantum interpretation is required at this stage: φ remains a classical continuum variable and ω_0 represents the characteristic restoring frequency. Its connection with relativistic quantum dynamics is introduced later through the Planck–Einstein relation.

For finite depletion, the equilibrium coefficients in Eq. (4.3) are replaced by the state-dependent responses derived in Sec. III.B,

$$\mu(\Phi) = \mu_0 f, \qquad T(\Phi) = T_0 f \tag{4.10}$$

Their common dependence preserves

$$\frac{T(\Phi)}{\mu(\Phi)} = c^2 \tag{4.11}$$

The present subsection therefore establishes the linear variational dynamics about the homogeneous vacuum, while the limiting static, propagating, and localized regimes are considered in Sec. IV.B. The consequences of the state-dependent response for finite depletion and strong gravitational fields are developed separately in Sec. V.

B. Limiting Cases of the Unified Continuum Equation

The master continuum equation derived in Sec. IV.A,

$$\mu_0\frac{\partial^2\varphi}{\partial t^2} - T_0\nabla^2\varphi + \frac{dU}{d\varphi} = J, \tag{4.12}$$

provides a unified description of small vacuum-capacity disturbances about the homogeneous state. Depending on the relative importance of the inertial, elastic, restoring, and loading terms, Eq. (4.12) reduces to several physically important limits. Such reductions are standard in continuum and variational dynamics [28, 32, 36].

(a) Static gravitational limit. For a stationary configuration, $\partial_t \varphi = 0$, and for long-range equilibrium redistribution the local restoring term may be neglected. Equation (4.12) then becomes

$$-T_0 \nabla^2 \varphi = J \tag{4.13}$$

Since $\varphi = c^2 - \Phi$, one has $\nabla^2 \varphi = -\nabla^2 \Phi$. Using the weak-field source normalization $J = 4\pi G T_0 \rho$, Eq. (4.13) gives

$$\nabla^2 \Phi = 4\pi G \rho, \tag{4.14}$$

which is precisely the static field equation obtained in Sec. III.A. Thus, Newtonian gravitation appears as the equilibrium limit of the same continuum dynamics. At finite depletion, the elastic response becomes state dependent, $T = T_0 f$, and the corresponding nonlinear redistribution is developed in Sec. V.

(b) Free-wave limit. In the absence of external loading and local restoring forces, $J = 0$ and $dU/d\varphi = 0$, Eq. (4.12) reduces to

$$\mu_0 \frac{\partial^2 \varphi}{\partial t^2} - T_0 \nabla^2 \varphi = 0 \tag{4.15}$$

Using $T_0/\mu_0 = c^2$, this becomes

$$\frac{\partial^2 \varphi}{\partial t^2} - c^2 \nabla^2 \varphi = 0 \tag{4.16}$$

Equation (4.16) is the standard wave equation for small disturbances in the continuum [28, 32] [2,3]. The characteristic propagation speed is therefore c. Under finite depletion, both available response coefficients acquire the same factor f, as derived in Sec. III.B, so their ratio remains $T/\mu = c^2$; consequently, the local characteristic propagation speed remains unchanged.

(c) Localized oscillatory limit. For a localized excitation whose spatial variation is negligible over the region of interest, $\nabla \varphi \simeq 0$. In the small-amplitude regime, the restoring potential of Sec. IV.A is

$$U(\varphi) \simeq \frac{1}{2} \mu_0 \omega_0^2 \varphi^2 \tag{4.17}$$

Equation (4.12) therefore becomes

$$\frac{\partial^2 \varphi}{\partial t^2} + \omega_0^2 \varphi = \frac{J}{\mu_0} \tag{4.18}$$

For a freely oscillating localized configuration, $J = 0$, giving

$$\frac{\partial^2 \varphi}{\partial t^2} + \omega_0^2 \varphi = 0 \tag{4.19}$$

Thus, a localized vacuum-capacity disturbance supports an intrinsic harmonic oscillation about equilibrium. At this stage, ω_0 is a classical continuum frequency determined by the restoring dynamics. The later identification $\hbar\omega_0 = mc^2$ introduces the relativistic energy scale and provides the connection with matter-wave dynamics. A Klein–Gordon-type equation can arise already at the level of a classical scalar field, before quantization, so the appearance of this mathematical structure here does not itself imply quantum mechanics [36].

The limiting cases therefore show that the same master continuum equation contains three distinct regimes: static redistribution reproduces the weak-field gravitational equation, source-free disturbances propagate with characteristic speed c, and localized disturbances support intrinsic oscillations. The finite-capacity relations derived in Sec. III.B need not be reintroduced here; they enter the subsequent theory through the state-dependent coefficients governing nonlinear vacuum redistribution in Sec. V.

V. Nonlinear Vacuum Response and Strong-Field Limit

A. State-Dependent Vacuum Redistribution

The linear formulation developed in Secs. III and IV applies to small departures from the homogeneous vacuum, for which the continuum response is characterized by the equilibrium coefficients μ_0 and T_0. At finite depletion, however, the locally available vacuum capacity decreases and the corresponding inertial and elastic responses become state dependent. From the capacity-partition relation established in Sec. III.B, these coefficients are

$$\mu(\Phi) = \mu_0 f,\ T(\Phi) = T_0 f,\ f = \frac{\Phi}{c^2} \tag{5.1}$$

Because the same depletion factor multiplies both response coefficients, their ratio remains unchang$\frac{T(\Phi)}{\mu(\Phi)} = \frac{T_0}{\mu_0} = c^2$. Finite depletion therefore modifies the magnitude of the available continuum response while preserving its characteristic propagation scale. The nonlinear behavior arises from the dependence of the response itself on the local vacuum state, rather than from the introduction of an independent strong-field interaction [28, 32, 37, 38].

The continuum dynamics of Sec. IV may be expressed in the flux-divergence form

$$\mu\frac{\partial^2\varphi}{\partial t^2} - \nabla\cdot(T\nabla\varphi) + \frac{dU}{d\varphi} = J \tag{5.2}$$

For a spatially uniform elastic response, $\nabla\cdot(T\nabla\varphi) = T\nabla^2\varphi$, and Eq. (5.2) reduces to the linear equation of Sec. IV. When T varies with the local vacuum state, the redistribution term instead satisfies

$$\nabla\cdot(T\nabla\varphi) = T\nabla^2\varphi + \nabla T\cdot\nabla\varphi \tag{5.3}$$

The additional gradient contribution is absent in the homogeneous limit and represents the modification of spatial redistribution produced by the state-dependent continuum response.

For static gravitational configurations, the temporal term vanishes. Restricting to the redistribution sector, for which the local oscillatory restoring contribution is absent, Eq. (5.2) becomes

$$-\nabla \cdot (T\nabla\varphi) = J \tag{5.4}$$

Since $\varphi = c^2 - \Phi$, one has $\nabla\varphi = -\nabla\Phi$, and hence

$$\nabla \cdot (T\nabla\Phi) = J \tag{5.5}$$

In the weak-depletion limit $T \to T_0$, Eq. (5.5) reduces to $T_0\nabla^2\Phi = J$. The source normalization established by matching to the Newtonian weak-field limit is

$$J = 4\pi G T_0 \rho \tag{5.6}$$

For finite depletion, substitution of $T = T_0 f$ into Eq. (5.5), followed by use of Eq. (5.6), gives

$$\nabla \cdot (f\nabla\Phi) = 4\pi G\rho \tag{5.7}$$

Equation (5.7) constitutes the nonlinear static redistribution equation of the bounded-vacuum framework. Using $f = \Phi/c^2$, it can equivalently be written as

$$\nabla \cdot \left(\frac{\Phi}{c^2}\nabla\Phi\right) = 4\pi G\rho \tag{5.8}$$

Expansion of the divergence yields

$$\Phi\nabla^2\Phi + |\nabla\Phi|^2 = 4\pi G c^2 \rho \tag{5.9}$$

The gradient-squared term in Eq. (5.9) has no counterpart in the linear theory. It appears because the capacity available to transmit the redistribution is itself controlled by the local field Φ. The strong-field nonlinearity therefore originates from the state dependence of the vacuum response while preserving the underlying local balance structure [28, 32, 37, 38].

The weak-field limit follows directly by writing $\Phi = c^2 + \phi_N$, with $|\phi_N|/c^2 \ll 1$. Substitution into Eq. (5.9) shows that $\phi_N\nabla^2\phi_N$and $|\nabla\phi_N|^2$are second order in the perturbation. Retaining only first-order terms therefore gives $\nabla^2\phi_N = 4\pi G\rho$. Thus, the nonlinear redistribution equation continuously reduces to the standard Poisson equation in the weak-field regime.

It is convenient to introduce an auxiliary redistribution potential Ψdefined by

$$\frac{d\Psi}{d\Phi} = f(\Phi) \tag{5.10}$$

For $f = \Phi/c^2$, integration gives

$$\Psi(\Phi) = \frac{\Phi^2}{2c^2} + C \tag{5.11}$$

Since $\nabla\Psi = f\nabla\Phi$, Eq. (5.7) becomes

$$\nabla^2\Psi = 4\pi G\rho \tag{5.12}$$

The nonlinear character of the physical vacuum-capacity field is therefore encoded in the constitutive relation between $\Psi$and Φ, whereas the redistribution equation expressed in terms of Ψretains the Poisson form. In the weak-field limit, $\Psi = c^2/2 + \phi_N + O(\phi_N^2/c^2)$; apart from an irrelevant additive constant, Ψtherefore approaches the Newtonian gravitational potential.

Equations (5.1)–(5.12) extend the linear vacuum-redistribution framework into the finite-depletion regime through the state dependence $T = T_0 f$and $\mu = \mu_0 f$. No separate strong-field force law is introduced. The resulting nonlinearity follows from the reduction of the locally available continuum response itself, while the common scaling of T and μ preserves the characteristic propagation scale c. The corresponding spherically symmetric exterior solution and its strong-field behavior are developed in Sec. V.B.

B. Spherically Symmetric Strong-Field Solution

The nonlinear equilibrium equation derived in Sec. V.A is

$$\nabla\cdot(f\nabla\Phi) = 4\pi G\rho, \qquad f = \frac{\Phi}{c^2} \tag{5.13}$$

Outside a localized spherically symmetric configuration, $\rho = 0$. For $\Phi = \Phi(r)$, Eq. (5.13) therefore becomes

$$\frac{1}{r^2}\frac{d}{dr}\left(r^2 f\frac{d\Phi}{dr}\right) = 0 \tag{5.14}$$

Integrating once gives $r^2 f\, d\Phi/dr = C$. Matching to the weak-field exterior solution $\Phi \simeq c^2 - Gm/r$ at large r, where $f \to 1$, fixes $C = Gm$. Hence,

$$r^2\frac{\Phi}{c^2}\frac{d\Phi}{dr} = Gm \tag{5.15}$$

Integration with the boundary condition $\Phi \to c^2$ as $r \to \infty$ gives

$$\Phi^2(r) = c^4\left(1 - \frac{2Gm}{rc^2}\right), \tag{5.16}$$

and therefore the physical exterior branch is

$$\Phi(r) = c^2\sqrt{1 - \frac{2Gm}{rc^2}}, \qquad f(r) = \sqrt{1 - \frac{2Gm}{rc^2}} \tag{5.17}$$

Thus,

$$f^2(r) = 1 - \frac{2Gm}{rc^2} \tag{5.18}$$

For $Gm/(rc^2) \ll 1$, expansion of Eq. (5.17) gives

$$\Phi(r) = c^2 - \frac{Gm}{r} - \frac{G^2m^2}{2r^2c^2} + O\left(\frac{G^3m^3}{r^3c^4}\right), \tag{5.19}$$

whose leading term is precisely the linear weak-field solution of Sec. III.

The same result follows directly from the auxiliary potential $\Psi = \Phi^2/(2c^2)$. Since $\nabla^2\Psi = 0$ outside the localized configuration, asymptotic matching gives

$$\Psi(r) = \frac{c^2}{2} - \frac{Gm}{r}, \tag{5.20}$$

which immediately reproduces Eq. (5.16). Thus, the auxiliary field retains the inverse-distance form while the physical vacuum-capacity field acquires the nonlinear square-root dependence.

The lower capacity bound $\Phi = 0$ is reached at

$$r_h = \frac{2Gm}{c^2} \tag{5.21}$$

This radius differs from the linear estimate $L_c = Gm/c^2$ of Sec. III.B because the latter was obtained by extrapolating the weak-field solution into the finite-depletion regime. The nonlinear solution instead places complete depletion at $2Gm/c^2$, numerically coinciding with the Schwarzschild radius of a static, spherically symmetric mass[1, 4, 39]. In general relativity, $2Gm/c^2$ is the Schwarzschild horizon radius.

Equation (5.17) is an exterior solution. Its direct continuation below r_h would make Φ imaginary, indicating that the present real-valued static capacity description does not determine the region $r < r_h$. An interior or saturated-vacuum solution must therefore be treated separately rather than inferred by extrapolating Eq. (5.17).

The central strong-field result is consequently

$$\boxed{\frac{\Phi^2(r)}{c^4} = f^2(r) = 1 - \frac{2Gm}{rc^2}.} \tag{5.22}$$

Remarkably, the same radial function appears in the Schwarzschild exterior geometry [1, 4, 39]. In the present framework, however, Eq. (5.22) arises from the state-dependent redistribution of the bounded vacuum rather than from Einstein's field equations. Its connection with the effective spacetime metric is developed in Sec. VI.

VI. Emergent Spacetime Structure from Vacuum Capacity

A. Temporal Scaling and Gravitational Time Dilation

The nonlinear solution of Sec. V establishes the normalized field $f = \Phi/c^2$ as the local measure of the remaining vacuum capacity. In the present framework, spacetime geometry is not introduced as an independent fundamental field; rather, the effective temporal and spatial scales are associated with the local vacuum-capacity state. We first consider the temporal sector.

Physical clocks measure time through the phase evolution of periodic processes. For a localized excitation of invariant rest mass m, define the reference proper-time oscillation frequency

$$\omega_0 = \frac{mc^2}{\hbar} \tag{6.1}$$

This frequency characterizes the locally measured intrinsic oscillation and therefore remains associated with the invariant rest energy mc^2. In a spatially varying vacuum-capacity field, the corresponding frequency measured relative to the asymptotic coordinate time is redshifted according to

$$\omega(\boldsymbol{x}) = f(\boldsymbol{x})\omega_0 = \frac{\Phi(x)}{c^2}\omega_0 \tag{6.2}$$

Equivalently,

$$\hbar\omega(\boldsymbol{x}) = mc^2 f(\boldsymbol{x}) = m\Phi(\boldsymbol{x}) \tag{6.3}$$

Equation (6.3) should be interpreted as the coordinate-associated energy/frequency scale, not as a variation of the locally measured invariant rest mass.

If θ denotes the oscillator phase, the same physical phase increment may be expressed relative to coordinate time as

$$d\theta = \omega(\boldsymbol{x})\, dt \tag{6.4}$$

or in terms of the invariant reference frequency and local proper time as

$$d\theta = \omega_0\, d\tau \tag{6.5}$$

Since phase is a physical invariant, equating Eqs. (6.4) and (6.5) and using Eq. (6.2) gives

$$d\tau = f(\boldsymbol{x})\, dt = \frac{\Phi(x)}{c^2}\, dt \tag{6.6}$$

Thus, the relation between local proper time and the asymptotic coordinate time is determined directly by the vacuum-capacity field. The corresponding temporal metric component is

$$g_{tt} = -f^2, \quad ds^2_{time} = -f^2 c^2 dt^2 \tag{6.7}$$

The nonlinear exterior solution obtained in Sec. V,

$$f^2(r) = 1 - \frac{2Gm}{rc^2}, \tag{6.8}$$

therefore gives

$$d\tau = \sqrt{1 - \frac{2Gm}{rc^2}}\, dt, \tag{6.9}$$

which is precisely the gravitational time-dilation factor of the Schwarzschild exterior geometry [1, 4, 39]. In the bounded-vacuum framework, however, this factor is interpreted as emerging from the spatial variation of the vacuum-capacity field.

The gravitational redshift follows from the same phase relation. For a stationary clock at radius r, the frequency referred to the asymptotic coordinate time is $\omega(r) = f(r)\omega_0$. Hence, for two stationary positions,

$$\frac{\omega(r_1)}{\omega(r_2)} = \frac{f(r_1)}{f(r_2)} = \sqrt{\frac{1-2Gm/(r_1c^2)}{1-2Gm/(r_2c^2)}} \tag{6.10}$$

For an observer at infinity, $f(\infty) = 1$, giving $\omega_\infty = f(r)\omega_{local}$, which reproduces the standard gravitational redshift relation [1, 4, 39].

The same capacity scaling also suggests the corresponding spatial normalization. For a locally propagating phase disturbance with characteristic speed c, the coordinate wave number satisfies

$$k(\boldsymbol{x}) = \frac{\omega(x)}{c} = k_0 f(\boldsymbol{x}), \qquad k_0 = \frac{\omega_0}{c} \tag{6.11}$$

The associated coordinate wavelength is therefore

$$\lambda(\boldsymbol{x}) = \frac{2\pi}{k(\boldsymbol{x})} = \frac{\lambda_0}{f(\boldsymbol{x})} \tag{6.12}$$

Since physical length standards can ultimately be related to microscopic wavelengths or periodic spatial standards, this reciprocal scaling motivates the local radial spatial relation

$$dl_{phys} = f^{-1}dl \tag{6.13}$$

Accordingly, the temporal and radial spatial sectors scale reciprocally,

$$d\tau = fdt,\ dl_{phys} = f^{-1}dl \tag{6.14}$$

This reciprocal relation provides the physical motivation for the effective metric construction developed explicitly in Sec. VI.B. It should be emphasized, however, that the spatial relation in Eq. (6.13) is a model assumption motivated by the proposed wavelength/ruler correspondence; unlike the temporal redshift relation, it does not follow from phase invariance alone.

In the weak-field regime, $Gm/(rc^2) \ll 1$,

$$f(r) = \sqrt{1 - \frac{2Gm}{rc^2}} \simeq 1 - \frac{Gm}{rc^2}, \tag{6.15}$$

so that

$$d\tau \simeq \left(1 - \frac{Gm}{rc^2}\right) dt = \left(1 + \frac{\phi_N}{c^2}\right) dt, \tag{6.16}$$

where $\phi_N = -Gm/r$. This is the standard weak-field gravitational time-dilation relation [1].

At the capacity boundary $r_h = 2Gm/c^2$, the exterior solution gives $f \to 0$, and consequently $d\tau/dt \to 0$ relative to the asymptotic Schwarzschild time coordinate. The temporal sector therefore follows from the phase evolution of localized vacuum excitations together with the spatially varying capacity field. The nonlinear solution of Sec. V reproduces the Schwarzschild gravitational time-dilation factor, while the reciprocal spatial scaling motivated above provides the basis for constructing the complete exterior metric in Sec. VI.B.

B. Spatial Scaling, Effective Refractive Index, and Emergent Schwarzschild Geometry

The temporal scaling obtained in Sec. VI.A, $d\tau = f dt$, determines the effective time component of the metric. The corresponding radial spatial scaling follows from the reciprocal wavelength relation established there,

$$dl_{\text{phys}} = f^{-1} dr \tag{6.17}$$

For a static spherically symmetric configuration, the radial coordinate r is chosen as the areal radius, so that spheres have physical area $4\pi r^2$. The angular sector therefore retains its standard form $r^2 d\Omega^2$, where

$$d\Omega^2 = d\theta^2 + \sin^2\theta \, d\phi^2 \tag{6.18}$$

Applying the reciprocal capacity scaling to the radial element gives

$$dl_{phys}^2 = f^{-2}(r) dr \tag{6.19}$$

Combining the temporal and spatial scaling relations yields the effective exterior line element

$$ds^2 = -f^2(r) c^2 dt^2 + f^{-2}(r) dr^2 + r^2 d\Omega^2 \tag{6.20}$$

The physical construction underlying Eq. (6.20) is illustrated schematically in Fig. 2. A reduction of the remaining vacuum capacity $f = \Phi/c^2$ produces the complementary temporal and radial scaling relations $d\tau = f dt$ and $dl_{\text{phys}} = f^{-1} dr$. These relations define the effective spacetime geometry while preserving the locally measured propagation speed c. Substitution of the nonlinear exterior capacity profile derived in Sec. V then yields the Schwarzschild exterior geometry, together with the associated gravitational time dilation, redshift, and light deflection.

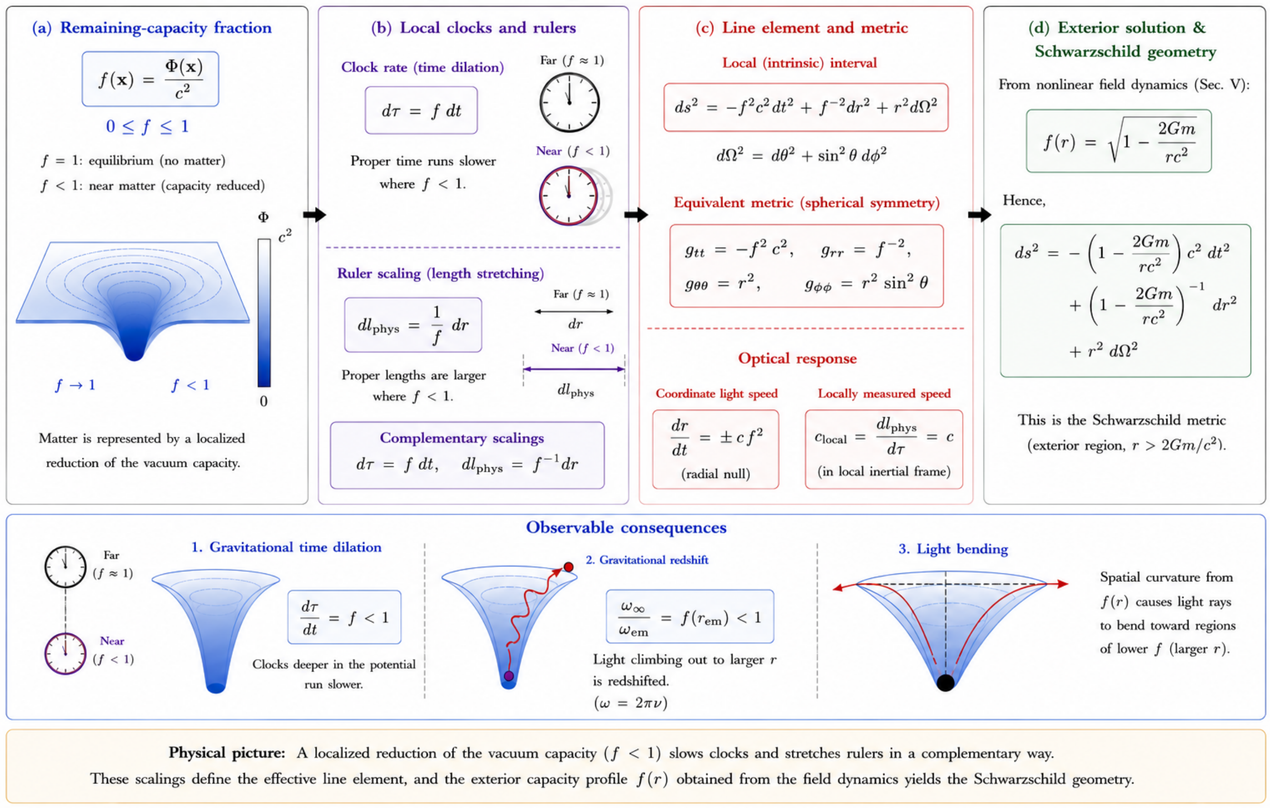

Figure 2. *Vacuum-capacity scaling and the emergence of effective spacetime geometry.*

Substituting the strong-field solution

$$f^2(r) = 1 - \frac{2Gm}{rc^2} \tag{6.21}$$

into Eq. (6.20) gives

$$ds^2 = -\left(1 - \frac{2Gm}{rc^2}\right)c^2dt^2 + \left(1 - \frac{2Gm}{rc^2}\right)^{-1} dr^2 + r^2 d\Omega^2 \tag{6.22}$$

Explicitly,

$$ds^2 = -\left(1 - \frac{2Gm}{rc^2}\right)c^2dt^2 + \left(1 - \frac{2Gm}{rc^2}\right)^{-1} dr^2 + r^2 d\theta^2 + r^2 \sin^2\theta\, d\phi^2 \tag{6.23}$$

Equation (6.23) is mathematically identical to the Schwarzschild exterior metric for a static, spherically symmetric, nonrotating mass[1, 4, 39]. The distinction is interpretational: in GR the Schwarzschild geometry is obtained from Einstein's field equations, whereas here the same exterior geometry is reconstructed from the nonlinear vacuum-capacity profile together with the temporal and spatial scaling relations.

An immediate consistency relation is

$$g_{tt}g_{rr} = -1 \tag{6.24}$$

For radial null propagation, $ds^2 = d\Omega^2 = 0$, Eq. (6.20) gives

$$\frac{dr}{dt} = \pm c f^2(r) \tag{6.25}$$

This is a coordinate velocity relative to r and t, not the locally measured velocity of light. Indeed, using $d\tau = f dt$ and $dl_{phys} = dr/f$,

$$\frac{dl_{phys}}{d\tau} = c \tag{6.26}$$

Thus, light always propagates locally at c, consistent with the continuum relation $T/\mu = c^2$.

The same result admits a useful optical interpretation. Relative to the asymptotic coordinates, Eq. (6.25) defines a radial effective refractive factor

$$n_r(r) \equiv \frac{c}{|dr/dt|} = \frac{1}{f^2(r)} = \left(1 - \frac{2Gm}{rc^2}\right)^{-1} \tag{6.27}$$

This quantity should be understood as an effective gravitational optical index, not as a material refractive index of the vacuum: the locally measured light speed remains exactly c. Moreover, because r is the Schwarzschild areal coordinate, Eq. (6.27) describes radial coordinate propagation and should not by itself be treated as an isotropic refractive index for arbitrary rays [26, 40, 41].

In the weak-field limit, $\epsilon = Gm/(rc^2) \ll 1$,

$$n_r(r) \simeq 1 + \frac{2Gm}{rc^2} \tag{6.28}$$

The factor of two is important. It reflects the combined temporal and spatial gravitational scaling. In an equivalent weak-field optical-metric description, the same first-order effective index governs light propagation [26, 40, 41]. For a ray passing a mass with impact parameter b, write $r = \sqrt{b^2 + z^2}$. The small-angle deflection obtained from the transverse gradient of the effective index is

$$\alpha \simeq \int_{-\infty}^{\infty} \frac{\partial n}{\partial b}\, dz \tag{6.29}$$

Using

$$n(r) \simeq 1 + \frac{2Gm}{c^2 r}, \tag{6.29}$$

gives, in magnitude,

$$\alpha = \frac{2Gm}{c^2} \int_{-\infty}^{\infty} \frac{b\, dz}{(b^2+z^2)^{3/2}} = \frac{4Gm}{bc^2} \tag{6.30}$$

Equation (6.30) is the standard first-order light-deflection angle of GR [1, 4, 26]. The result is twice the Newtonian corpuscular value $2Gm/(bc^2)$; in the present construction, the full factor arises because the vacuum-capacity field determines both the temporal scaling $d\tau = f dt$ and the reciprocal spatial scaling $dl_{phys} = f^{-1} dl$.

The weak-field metric correspondingly satisfies

$$g_{tt} \simeq -\left(1-\frac{2Gm}{rc^2}\right), \qquad g_{rr} \simeq 1+\frac{2Gm}{rc^2}, \tag{6.31}$$

reproducing the first-order Schwarzschild behavior. Since the complete metric (6.22) is Schwarzschild, the associated gravitational redshift, light deflection, Shapiro delay, perihelion advance, and other exterior geodesic predictions are identical to those of GR within the static spherical sector [4, 26].

At the capacity boundary

$$r_h = \frac{2Gm}{c^2}, \tag{6.32}$$

one has $f \to 0$, $g_{tt} \to 0$, and $g_{rr} \to \infty$ in Schwarzschild coordinates. Correspondingly, the coordinate optical factor $n_r = 1/f^2$ diverges. This does not represent a vanishing local light speed; Eq. (6.26) continues to express the local causal propagation speed c. The boundary instead corresponds to the infinite redshift and coordinate-time behavior of the Schwarzschild exterior representation [4]. The present exterior construction does not by itself determine the continuation of the vacuum-capacity field into $r < r_h$.

The central geometrical result remains

$$\boxed{ds^2 = -f^2c^2dt^2 + f^{-2}dr^2 + r^2 d\Omega^2, \qquad f^2 = 1-\frac{2Gm}{rc^2}.}$$

VII. Relativistic Phase and Matter-Wave Dynamics of Localized Vacuum Excitations

A. Intrinsic Vacuum Oscillation and Emergence of the Relativistic Matter-Wave Phase

The continuum dynamics developed in Sec. IV admit localized oscillatory vacuum-capacity excitations. In the localized limit, where spatial gradients may be neglected, the source-free equation reduces to

$$\frac{d^2\varphi}{d\tau^2} + \omega_0^2\varphi = 0, \tag{7.1}$$

where τ is the proper time of the localized excitation and ω_0 is its intrinsic rest-frame frequency. The corresponding solution may be written as $\varphi(\tau) = A\cos(\omega_0\tau + \theta_0)$, with intrinsic phase

$$\theta = \omega_0\tau \tag{7.2}$$

Thus, within the present framework, a material excitation possesses an intrinsic periodic dynamics arising from the localized oscillation of the vacuum-capacity deficit rather than from an independently introduced matter wave.

To connect this continuum oscillation with the observed relativistic energy scale, we impose the Planck–Einstein normalization [18, 42].

$$\hbar\omega_0 = mc^2, \qquad \omega_0 = \frac{mc^2}{\hbar} \tag{7.3}$$

Here m is the invariant mass identified with the localized vacuum loading in the preceding sections. Equation (7.3) provides the quantum normalization of the intrinsic continuum oscillation; the appearance of $\hbar$ is therefore an input connecting the bounded-vacuum dynamics to the experimentally established energy-frequency relation rather than a quantity derived from the classical continuum action itself [42].

Because the physical phase is a Lorentz scalar, the same phase observed from an inertial frame in which the localized excitation moves with velocity $\boldsymbol{v}$ may be written as [18, 36, 43].

$$\theta = \omega t - \boldsymbol{k} \cdot \boldsymbol{x} \tag{7.4}$$

Equating this expression with the proper-time phase $\theta = \omega_0 \tau$, or equivalently Lorentz transforming the rest-frame phase four-vector $K_0^\mu = (\omega_0/c, \mathbf{0})$, gives

$$\omega = \gamma\omega_0, \qquad \boldsymbol{k} = \gamma \frac{\omega_0}{c^2} \boldsymbol{v}, \tag{7.5}$$

where $\gamma = (1 - v^2/c^2)^{-1/2}$.

Using Eq. (7.3), these relations become

$$\hbar\omega = \gamma m c^2, \qquad \hbar\boldsymbol{k} = \gamma m \boldsymbol{v} \tag{7.6}$$

Identifying the relativistic energy and momentum of the localized excitation as $E = \gamma mc^2$ and $\boldsymbol{p} = \gamma m \boldsymbol{v}$ therefore yields

$$E = \hbar\omega, \qquad \boldsymbol{p} = \hbar\boldsymbol{k} \tag{7.8}$$

The associated spatial wavelength is consequently

$$\lambda_{dB} = \frac{2\pi}{k} = \frac{h}{p} \tag{7.9}$$

which is the de Broglie relation[18, 42, 44]. In this interpretation, the de Broglie wave is the spatial phase structure generated when the intrinsic oscillation of a moving localized vacuum excitation is described in an inertial frame. It is therefore distinct from the physical localization size of the underlying vacuum deficit.

B. Relativistic Dispersion, Klein–Gordon Limit, and Causal Propagation

The relativistic phase obtained in Sec. VII.A connects the intrinsic oscillation of a localized vacuum excitation with its spacetime propagation. Since the phase four-vector $K^\mu = (\omega/c, \boldsymbol{k})$ is related by a Lorentz transformation to the rest-frame vector $K_0^\mu = (\omega_0/c, \mathbf{0})$, its invariant norm satisfies [18, 36, 43]

$$\frac{\omega^2}{c^2} - k^2 = \frac{\omega_0^2}{c^2},$$

and therefore

$$\omega^2 = c^2 k^2 + \omega_0^2 \tag{7.9}$$

Importantly, Eq. (7.9) is also obtained directly from the source-free bounded-vacuum continuum equation derived in Sec. IV,

$$\frac{1}{c^2}\frac{\partial^2\varphi}{\partial t^2} - \nabla^2\varphi + \frac{\omega_0^2}{c^2}\varphi = 0 \tag{7.10}$$

For a normal mode $\varphi = Ae^{i(\boldsymbol{k}\cdot\boldsymbol{x}-\omega t)}$, Eq. (7.10) gives precisely the dispersion relation (7.9). Thus, the Lorentz transformation of the localized vacuum oscillation and the independently derived continuum dynamics possess the same relativistic dispersion structure.

Using the quantum normalization $\omega_0 = mc^2/\hbar$ established in Sec. VII.A, Eq. (7.9) becomes

$$\hbar^2\omega^2 = \hbar^2c^2k^2 + m^2c^4 \tag{7.11}$$

With $E = \hbar\omega$ and $\boldsymbol{p} = \hbar\boldsymbol{k}$, this yields

$$E^2 = p^2c^2 + m^2c^4, \tag{7.12}$$

recovering the relativistic energy-momentum relation[18, 36, 43, 45]. Correspondingly, Eq. (7.10) becomes

$$\frac{1}{c^2}\frac{\partial^2\varphi}{\partial t^2} - \nabla^2\varphi + \frac{m^2c^2}{\hbar^2}\varphi = 0, \tag{7.13}$$

or

$$\left(\Box + \frac{m^2c^2}{\hbar^2}\right)\varphi = 0, \tag{7.14}$$

which has the standard free Klein–Gordon form [44-46]. In the present framework, however, φ originates as the oscillatory vacuum-capacity deficit, so the Klein–Gordon structure follows from the bounded-vacuum continuum after imposing the quantum normalization of its intrinsic frequency.

The dispersion relation also constrains the propagation velocity. Differentiating Eq. (7.9) gives the group velocity

$$v_g = \frac{d\omega}{dk} = \frac{c^2k}{\sqrt{c^2k^2+\omega_0^2}} \tag{7.15}$$

For a massive excitation, $\omega_0 > 0$, and therefore

$$v_g^2 = c^2\frac{c^2k^2}{c^2k^2+\omega_0^2} < c^2,$$

so that

$$v_g < c \tag{7.16}$$

Using $p = \hbar k$ and $E = \hbar\omega$, this is equivalently $v_g = pc^2/E = v$. Thus, a massive localized vacuum excitation cannot propagate superluminally. In the high-wave-number limit $ck \gg \omega_0$, $v_g \to c$ from below but never exceeds c.

For a massless disturbance, $\omega_0 = 0$, Eq. (7.9) reduces to

$$\omega = ck, \qquad v_g = c$$

Hence, within the lowest-order bounded-vacuum continuum considered here, massless disturbances propagate nondispersively at c, whereas massive localized excitations propagate subluminally. Although the phase velocity of a massive mode is $v_{\mathrm{ph}} = \frac{\omega}{k} = c^2/v_g > c$, it does not represent transport of energy, matter, or information and therefore does not constitute superluminal propagation [36, 44].

VIII. Nonrelativistic and Localization Limits

A. Schrödinger Limit of the Vacuum-Excitation Dynamics

The relativistic vacuum-excitation equation obtained in Sec. VII.B,

$$\frac{1}{c^2}\frac{\partial^2\varphi}{\partial t^2} - \nabla^2\varphi + \frac{m^2c^2}{\hbar^2}\varphi = 0, \tag{8.1}$$

contains the rapid intrinsic oscillation $\omega_0 = mc^2/\hbar$ associated with the rest-energy scale. To obtain the nonrelativistic limit, the field may be represented by a complex positive-frequency component whose rapidly varying intrinsic phase is separated from a slowly varying envelope $\psi(\boldsymbol{x}, t)$ [44, 45, 47]:

$$\varphi(\boldsymbol{x}, t) = \psi(\boldsymbol{x}, t)e^{-i\omega_0 t} \tag{8.2}$$

For the underlying real vacuum-capacity deficit, the physical field may equivalently be taken as the real part of Eq. (8.2); the complex representation provides a convenient description of its phase and slowly varying envelope.

Substitution of Eq. (8.2) into Eq. (8.1), using $\omega_0 = mc^2/\hbar$, gives

$$\frac{1}{c^2}\frac{\partial^2\psi}{\partial t^2} - \frac{2i\omega_0}{c^2}\frac{\partial\psi}{\partial t} - \nabla^2\psi = 0 \tag{8.3}$$

In the nonrelativistic regime, the envelope varies slowly compared with the intrinsic oscillation, so that $|\partial_t^2\psi| \ll \omega_0|\partial_t\psi|$. Neglecting the first term of Eq. (8.3) therefore yields

$$-\frac{2i\omega_0}{c^2}\frac{\partial\psi}{\partial t} - \nabla^2\psi \simeq 0 \tag{8.4}$$

Using $\omega_0 = mc^2/\hbar$, Eq. (8.4) becomes

$$i\hbar\frac{\partial\psi}{\partial t} = -\frac{\hbar^2}{2m}\nabla^2\psi, \tag{8.5}$$

which is the free-particle Schrödinger equation [44, 45, 47].

Within the bounded-vacuum framework, ψ therefore represents the slowly varying complex envelope of the relativistic phase dynamics of a localized vacuum excitation after the rapid rest-frequency factor $e^{-imc^2t/\hbar}$ has been separated. Equation (8.5) is not introduced as an independent nonrelativistic postulate but arises as the low-energy limit of the relativistic continuum equation obtained in Sec. VII.

The same result follows directly from the BVT dispersion relation. Writing

$$\omega = \sqrt{\omega_0^2 + c^2k^2}, \tag{8.6}$$

and expanding for $ck \ll \omega_0$ gives

$$\omega \simeq \omega_0 + \frac{c^2k^2}{2\omega_0} \tag{8.7}$$

Removing the intrinsic rest oscillation leaves the envelope frequency $\Omega \equiv \omega - \omega_0$, for which

$$\hbar\Omega = \frac{\hbar^2k^2}{2m} = \frac{p^2}{2m} \tag{8.8}$$

Thus, the nonrelativistic kinetic-energy relation and the Schrödinger evolution arise from the same low-k expansion of the bounded-vacuum dispersion relation.

It should be emphasized that this derivation establishes the **dynamical Schrödinger limit** of the vacuum-excitation field. The probabilistic Born interpretation $P = |\psi|^2$, measurement postulates, and quantization of interacting fields do not follow from Eq. (8.5) alone and would require additional physical structure [6, 44].

B. Compton Localization and the Planck Scale

The intrinsic oscillation introduced in Sec. VII provides a natural length scale for a localized vacuum excitation. Since the characteristic propagation speed of the bounded-vacuum continuum is c, the intrinsic frequency $\omega_0 = mc^2/\hbar$ defines the reduced Compton scale

$$\ell_C \equiv \frac{c}{\omega_0} = \frac{\hbar}{mc} \tag{8.9}$$

Thus, ℓ_C represents the distance over which a disturbance propagating at c accumulates an intrinsic phase of order unity. The full phase wavelength is $\lambda_C = 2\pi\ell_C = h/(mc)$. The Compton wavelength is the standard relativistic quantum localization scale associated with a particle of mass m [6, 44, 45, 48].

Within the present framework, ℓ_C should not be identified automatically with the physical radius of the localized vacuum-deficit core. Rather, it characterizes the intrinsic phase/localization scale associated with the oscillatory excitation. Localization substantially below this scale requires momentum and energy sufficiently large that a fixed-particle-number description ceases to be adequate in relativistic quantum theory [6, 44, 45].

The bounded-vacuum description independently introduces a gravitational localization scale through the finite-capacity condition. As obtained in Sec. III.B, the linear estimate is

$$L_c = \frac{Gm}{c^2} \tag{8.10}$$

This scale marks the onset of strong vacuum depletion in the linear theory; it is not the exact strong-field horizon radius, which the nonlinear solution of Sec. V gives as $r_h = 2Gm/c^2$.

A characteristic crossover occurs when the quantum phase-localization scale and the gravitational depletion scale become comparable,

$$\ell_C \sim L_c \tag{8.11}$$

Using Eqs. (8.9) and (8.10),

$$\frac{\hbar}{mc} \sim \frac{Gm}{c^2},$$

which gives

$$m^2 \sim \frac{\hbar c}{G} \tag{8.12}$$

Hence the corresponding mass scale is

$$m \sim m_P \equiv \sqrt{\frac{\hbar c}{G}}, \tag{8.13}$$

and substitution into either length scale gives

$$\ell_P \equiv \sqrt{\frac{\hbar G}{c^3}} \tag{8.14}$$

These are the conventional Planck mass and Planck length [49-51]. In the bounded-vacuum interpretation, their appearance identifies the regime in which the characteristic quantum phase-localization scale becomes comparable to the scale at which gravitational vacuum depletion can no longer be treated perturbatively.

If instead the exact nonlinear capacity boundary $r_h = 2Gm/c^2$ is equated to the reduced Compton wavelength, the crossover differs only by an order-unity factor,

$$m = \sqrt{\frac{\hbar c}{2G}}, \qquad \ell = \sqrt{2}\,\ell_P \tag{8.15}$$

Accordingly, the robust result is the Planck scale, rather than a unique numerical crossover coefficient. This distinction is important because neither the Compton wavelength nor the gravitational radius defines a sharply localized particle boundary [6, 50, 51].

IX. Relativistic Quantum Dynamics in a Spatially Varying Vacuum-Capacity Field

The matter-wave dynamics of Secs. VII and VIII were developed for the homogeneous vacuum, $f = 1$. In a gravitational configuration, the remaining capacity varies as $f(\boldsymbol{x}) = \Phi(\boldsymbol{x})/c^2$, and the phase dynamics must be referred to the emergent spacetime structure obtained in Sec. VI. The intrinsic proper-time oscillation remains

$$d\theta = \omega_0\, d\tau, \qquad \omega_0 = \frac{mc^2}{\hbar} \tag{9.1}$$

For a stationary excitation, $d\tau = f\, dt$, and hence the frequency referred to the asymptotic coordinate time is

$$\omega(\boldsymbol{x}) = f(\boldsymbol{x})\omega_0, \qquad \hbar\omega(\boldsymbol{x}) = mc^2 f(\boldsymbol{x}) = m\Phi(\boldsymbol{x}) \tag{9.2}$$

Thus, $m\Phi$ represents the coordinate-associated energy scale of a stationary excitation, whereas its locally measured invariant rest energy remains mc^2. For moving excitations, the gravitational and kinematic effects are incorporated together through the covariant phase relation [36, 52]

$$d\theta = \frac{1}{\hbar} p_\mu dx^\mu = \omega_0 \, d\tau, \tag{9.3}$$

with the overall phase sign depending on convention. The corresponding mass-shell condition is

$$g^{\mu\nu} p_\mu p_\nu = -m^2 c^2 \tag{9.4}$$

Using the emergent BVT metric derived in Sec. VI,

$$ds^2 = -f^2 c^2 dt^2 + f^{-2} dr^2 + r^2 d\Omega^2, \tag{9.5}$$

the relativistic phase action S, defined through $\theta = S/\hbar$, satisfies the Hamilton–Jacobi equation

$$-\frac{1}{f^2 c^2}\left(\frac{\partial S}{\partial t}\right)^2 + f^2\left(\frac{\partial S}{\partial r}\right)^2 + \frac{1}{r^2}\left(\frac{\partial S}{\partial \theta}\right)^2 + \frac{1}{r^2 \sin^2\theta}\left(\frac{\partial S}{\partial \phi}\right)^2 + m^2 c^2 = 0 \tag{9.6}$$

Thus, the same capacity field f that determines temporal and spatial scaling also governs the relativistic phase propagation of the localized vacuum excitation.

The natural minimally coupled extension of the flat-space Klein–Gordon equation obtained in Sec. VII.B to this emergent geometry is [52-54]

$$\left(\Box_g - \frac{m^2 c^2}{\hbar^2}\right)\psi = 0, \tag{9.7}$$

where, using the $(-+++)$ signature,

$$\Box_g \psi \equiv \frac{1}{\sqrt{-g}} \partial_\mu\left(\sqrt{-g}\, g^{\mu\nu}\, \partial_\nu \psi\right) \tag{9.8}$$

Curved-spacetime Klein–Gordon dynamics are conventionally obtained by replacing the flat spacetime wave operator by its generally covariant counterpart. For Eq. (9.5), this gives

$$-\frac{1}{f^2 c^2}\frac{\partial^2 \psi}{\partial t^2} + \frac{1}{r^2}\frac{\partial}{\partial r}\left(r^2 f^2 \frac{\partial \psi}{\partial r}\right) + \frac{1}{r^2}\nabla_\Omega^2 \psi - \frac{m^2 c^2}{\hbar^2}\psi = 0 \tag{9.9}$$

Equation (9.9) should be regarded as the minimal-coupling extension of the BVT matter-wave dynamics to the emergent geometry rather than as an independent fundamental postulate. A complete derivation from BVT would require extending the continuum action of Sec. IV explicitly to the state-dependent spacetime background.

In the weak-field regime, $\Phi \simeq c^2 + \phi_N$, with $|\phi_N|/c^2 \ll 1$. Separating the rapid rest phase $e^{-imc^2 t/\hbar}$ and retaining the leading nonrelativistic terms reduces the relativistic dynamics to the gravitational Schrödinger equation [53-55]

$$i\hbar \frac{\partial \psi}{\partial t} = -\frac{\hbar^2}{2m}\nabla^2 \psi + m\phi_N \psi \tag{9.10}$$

The recovery of Schrödinger-type dynamics as the nonrelativistic weak-field limit of Klein–Gordon dynamics in a gravitational metric is standard. In the bounded-vacuum description,

$$\phi_N = \Phi - c^2, \qquad V_g = m(\Phi - c^2) \tag{9.11}$$

The gravitational potential energy therefore appears as the weak-field departure of the vacuum-capacity energy from its homogeneous value, while the full strong-field phase dynamics are governed by the emergent metric $g_{\mu\nu}(f)$.

X. Physical Consequences and Testable Predictions

The preceding sections show that the bounded-vacuum framework reproduces the Newtonian weak-field limit, Schwarzschild exterior geometry, relativistic matter-wave dispersion, and the nonrelativistic Schrödinger limit. Since the static spherically symmetric metric of Sec. VI is identical to the Schwarzschild exterior metric, conventional static gravitational tests cannot by themselves distinguish the present framework from General Relativity (GR). Distinguishing signatures must instead arise from the **dynamical response of the vacuum-capacity field**, particularly where $f = \Phi/c^2$ varies strongly in space or time.

A. Static Gravitational and Quantum Limits

For a weakly coupled test body, Sec. III gives

$$\boldsymbol{a} = -\nabla\Phi, \tag{10.1}$$

which is independent of the test-body mass. The bounded-vacuum theory therefore predicts universal free fall at the level developed here, consistent with experimental tests of the weak equivalence principle [25, 56, 57]. The MICROSCOPE experiment, for example, found no violation at approximately the 10^{-15} level.

Similarly, the nonlinear exterior solution

$$f^2(r) = 1 - \frac{2Gm}{rc^2} \tag{10.2}$$

produces

$$ds^2 = -\left(1 - \frac{2Gm}{rc^2}\right)c^2dt^2 + \left(1 - \frac{2Gm}{rc^2}\right)^{-1}dr^2 + r^2d\Omega^2 \tag{10.3}$$

Consequently, gravitational redshift, light deflection, Shapiro delay, perihelion advance, and other observables determined solely by the Schwarzschild exterior geometry agree with GR [39, 52, 58]. These constitute consistency requirements rather than unique predictions of the bounded-vacuum interpretation.

The matter-wave sector similarly recovers

$$E = \hbar\omega, \qquad p = \hbar k, \quad \lambda_{dB} = \frac{h}{p} \tag{10.4}$$

together with the weak-field gravitational potential energy

$$V_g = m(\Phi - c^2) \simeq m\phi_N \tag{10.5}$$

Thus, conventional matter-wave and weak-field interferometric phenomena are recovered at leading order[18, 44].

B. Propagation of Vacuum Disturbances

A more direct dynamical consequence follows from the bounded-vacuum continuum equation. In a homogeneous background, the dispersion relation derived in Sec. VII is

$$\omega^2 = c^2k^2 + \omega_0^2 \tag{10.6}$$

For massless vacuum disturbances, $\omega_0 = 0$, giving

$$\omega = ck, \qquad v_g = \frac{d\omega}{dk} = c \tag{10.7}$$

The lowest-order BVT continuum therefore predicts no frequency-dependent dispersion for massless propagation in a homogeneous vacuum. Superluminal signal propagation is likewise excluded: massive excitations satisfy $v_g < c$, whereas massless disturbances satisfy $v_g = c$.

This result is experimentally important because gravitational-wave observations strongly constrain modified propagation laws. Current gravitational-wave tests have found no evidence for anomalous dispersion, additional polarization modes, or departures from the relativistic propagation expected in GR [59]. Thus, the nondispersive massless limit of the present continuum is compatible with existing observations.

Any observable BVT departure in wave propagation would consequently have to originate from state-dependent dynamics in an inhomogeneous or strongly depleted vacuum, rather than from an arbitrary modification of the homogeneous dispersion relation. Such corrections should be derived from the nonlinear dynamical action before quantitative observational bounds are claimed.

C. Strong-Field Dynamical Signatures

The most promising distinction from GR arises because BVT assigns a physical continuum state to the quantity

$$f(r) = \sqrt{1 - \frac{2Gm}{rc^2}}, \tag{10.8}$$

which approaches zero near the capacity boundary. Although the stationary exterior metric coincides with Schwarzschild geometry, perturbations of the underlying capacity field need not possess exactly the same dynamical weighting as metric perturbations in GR.

If a dynamical perturbation $\delta\Phi$ is introduced about the equilibrium background,

$$\Phi(\boldsymbol{x}, t) = \bar{\Phi}(\boldsymbol{x}) + \delta\Phi(\boldsymbol{x}, t), \tag{10.9}$$

then the nonlinear response developed in Sec. V implies that its propagation coefficients depend on the background remaining capacity $\bar{f} = \bar{\Phi}/c^2$. Schematically, the perturbation equation therefore takes the form

$$\partial_t\left[\mu(\bar{f})\ \partial_t\delta\Phi\right] - \nabla \cdot \left[T(\bar{f})\nabla\delta\Phi\right] + \cdots = 0 \tag{10.10}$$

If the depletion rescales the two coefficients proportionally,

$$T(\bar{f}) = T_0\bar{f}, \qquad \mu(\bar{f}) = \mu_0\bar{f}, \tag{10.11}$$

then

$$\frac{T(\bar{f})}{\mu(\bar{f})} = \frac{T_0}{\mu_0} = c^2, \tag{10.12}$$

so the local characteristic propagation speed remains c. Nevertheless, spatial gradients of $\bar{f}$ remain in Eq. (10.10) and can modify the amplitude and effective perturbation potential without producing superluminal propagation or a frequency-dependent vacuum speed.

This identifies strong-field transient phenomena—particularly black-hole perturbations and ringdown—as a potentially useful testing regime. Existing gravitational-wave observations have so far found black-hole ringdown and other strong-field consistency tests compatible with GR [59]. A genuine BVT prediction would therefore require deriving the complete linearized perturbation equation about the nonlinear background and calculating its quasinormal-mode spectrum,

$$\omega_{QNM}^{BVT} = \omega_{QNM}^{GR} + \delta\omega(f) \tag{10.13}$$

with corresponding damping modification

$$\tau_{QNM}^{BVT} = \tau_{QNM}^{GR} + \delta\tau(f) \tag{10.14}$$

Equations (10.13) and (10.14) should presently be regarded as targets for a distinguishing prediction, rather than established deviations of the theory. This distinction is important because current gravitational-wave observations show no evidence for dispersion or significant departures of measured remnant/ringdown properties from GR expectations.

Accordingly, the experimentally relevant feature of the present framework is not a deviation from established weak-field or static Schwarzschild physics, but the possibility that the bounded capacity $0 \le f \le 1$ modifies the dynamical response of strongly depleted vacuum configurations while preserving the local causal speed c.

XI. Discussion and Limitations

The bounded-vacuum framework developed here provides an effective continuum description in which a single scalar field Φ, bounded by $0 \le \Phi \le c^2$, characterizes the local vacuum state. Localized depletion represents matter loading, while redistribution of the remaining capacity determines the gravitational response. The normalized field $f = \Phi/c^2$ consequently connects the nonlinear vacuum response to the effective temporal and spatial scaling derived in Secs. V and VI. In the static spherically symmetric exterior, this construction reproduces the Schwarzschild metric exactly. The agreement with General Relativity (GR) in this sector should therefore be regarded as a consistency result rather than a distinguishing prediction [4, 39, 58].

The matter-wave sector provides a second connection. The continuum action admits localized oscillatory excitations with intrinsic frequency ω_0. Upon imposing the experimentally established quantum normalization $\hbar\omega_0 = mc^2$, Lorentz transformation of the intrinsic phase yields the Planck–Einstein and de Broglie relations, while the continuum dispersion relation acquires the Klein–Gordon form and reduces to Schrödinger dynamics in the nonrelativistic limit[6, 18, 45, 46]. Thus, the framework supplies a common continuum interpretation of these gravitational and matter-wave structures, but it does not constitute a complete derivation of quantum mechanics.

Several ingredients remain assumptions or effective constructions rather than consequences derived from a microscopic theory. In particular, the scale $\hbar$ enters through the quantum normalization rather than being derived from the bounded-vacuum dynamics. The reciprocal spatial scaling used to construct the emergent metric is motivated by the proposed wavelength/ruler correspondence, while the curved-space Klein–Gordon equation of Sec. IX is the natural minimal-coupling extension of the flat-space continuum dynamics rather than the result of a fully state-dependent BVT action. A more complete formulation should derive these structures from a common dynamical principle.

The present analysis is also restricted mainly to scalar excitations and static spherical gravitational configurations. The physical continuation of the capacity field inside $r_h = 2Gm/c^2$, rotating and nonspherical configurations, spinor and gauge degrees of freedom, quantum measurement and the Born rule, and the microscopic structure responsible for vacuum capacity remain unresolved. These limitations distinguish the present construction from established complete frameworks such as GR and relativistic quantum field theory [4, 6, 7, 58].

A decisive assessment of the theory ultimately requires predictions that differ quantitatively from established physics. Because the static exterior metric coincides with Schwarzschild geometry and the homogeneous massless dispersion relation gives $v_g = c$, the most promising departures are expected in the dynamical response of strongly depleted vacuum configurations. Linear perturbations about the nonlinear capacity background, black-hole quasinormal modes, and gravitational-wave ringdown therefore provide natural directions for determining whether the bounded-vacuum dynamics produce observable deviations from GR [60, 61]. Until such deviations are derived and confronted with experiment, the present theory is most appropriately regarded as an effective continuum framework that provides a unified physical interpretation of several established gravitational and relativistic matter-wave limits.

XII. Conclusions

We have developed an effective continuum framework in which the vacuum is characterized by a bounded scalar capacity field $\Phi(x,t)$, with normalized remaining-capacity fraction $f = \Phi/c^2$. Matter is represented by localized depletion of this capacity, while gravitation arises from the associated redistribution of the remaining vacuum response. In the weak-field regime, the governing field equation recovers the Poisson equation and therefore Newtonian gravity. Beyond this limit, a capacity-dependent nonlinear response yields the exterior solution $\Phi(r) = c^2\sqrt{1 - 2Gm/(rc^2)}$, or equivalently $f(r) = \sqrt{1 - 2Gm/(rc^2)}$. When this local capacity fraction is related to temporal and reciprocal radial scaling, the corresponding exterior line element takes the Schwarzschild form,

$$ds^2 = -f^2c^2dt^2 + f^{-2}dr^2 + r^2d\Omega^2.$$

Thus, within the present framework, the Schwarzschild exterior geometry emerges from the spatial redistribution of the remaining vacuum capacity rather than being introduced independently as a prescribed spacetime geometry.

The same continuum description also admits localized oscillatory excitations. With the intrinsic quantum normalization

$$\hbar\omega_0 = mc^2,$$

Lorentz transformation of the rest-frame phase yields the Planck–Einstein and de Broglie relations together with the relativistic energy-momentum dispersion relation. The associated continuum wave dynamics acquire the Klein–Gordon form and reduce to the Schrödinger equation in the nonrelativistic limit. Massive excitations remain subluminal, while massless disturbances propagate nondispersively at the limiting speed c. In this way, the bounded-capacity field provides a common description linking matter localization, gravitational redistribution, emergent spacetime scaling, and relativistic matter-wave dynamics.

The framework should therefore be regarded as an effective continuum construction whose significance depends not only on reproducing established weak-field and exterior relativistic results, but also on whether it leads to physically distinguishable consequences. Particularly important tests concern the dynamical behavior of strongly depleted configurations, where the bounded nature of the vacuum capacity may become relevant, as well as extensions to nonspherical and rotating systems, time-dependent gravitational configurations, and quantum-field degrees of freedom. These regimes provide the natural setting for determining whether the bounded-vacuum description represents only an alternative formulation of known gravitational and relativistic dynamics or yields genuinely new observable predictions.

References:

1. Albert, E., W. Perrett, and G. Jeffery, *The foundation of the general theory of relativity*. Annalen der Physik, 1916. **354**(7): p. 769.
2. Will, C.M., *The confrontation between general relativity and experiment*. Living reviews in relativity, 2014. **17**(1): p. 4.
3. Abbott, B.P., et al., *Observation of gravitational waves from a binary black hole merger*. Physical review letters, 2016. **116**(6): p. 061102.
4. Misner, C.W., et al., *Gravitation*. Physics Today, 1974. **27**(8): p. 47-48.
5. Dirac, P.A., *Quantum mechanics*. 1958: Oxford University Press.[DRF].
6. Weinberg, S., *The quantum theory of fields*. Vol. 2. 1995: Cambridge university press.
7. Peskin, M.E., D.V. Schroeder, and E. Martinec, *An Introduction to quantum field theory*. 1996, American Institute of Physics.
8. Rovelli, C., *Quantum gravity*. Scholarpedia, 2008. **3**(5): p. 7117.
9. Thiemann, T., *Modern canonical quantum general relativity*. 2008: Cambridge University Press.
10. Ambj∅ rn, J., J. Jurkiewicz, and R. Loll, *The universe from scratch*. Contemporary Physics, 2006. **47**(2): p. 103-117.
11. Niedermaier, M. and M. Reuter, *The asymptotic safety scenario in quantum gravity*. Living Reviews in Relativity, 2006. **9**(5): p. 173.
12. Sakharov, A.D., *Vacuum quantum fluctuations in curved space and the theory of gravitation*. Usp. Fiz. Nauk, 1991. **161**(5): p. 64-66.
13. Jacobson, T., *Thermodynamics of spacetime: the Einstein equation of state*. Physical review letters, 1995. **75**(7): p. 1260.
14. Verlinde, E., *On the origin of gravity and the laws of Newton*. Journal of High Energy Physics, 2011. **2011**(4): p. 1-27.
15. Lamb Jr, W.E. and R.C. Retherford, *Fine structure of the hydrogen atom by a microwave method*. Physical Review, 1947. **72**(3): p. 241.
16. Greiner, W. and J. Reinhardt, *Quantum-Electrodynamical Processes*, in *Quantum Electrodynamics*. 2009, Springer. p. 77-241.
17. De Broglie, L., *Waves and quanta*. Nature, 1923. **112**(2815): p. 540-540.
18. De Broglie, L., *Recherches sur la théorie des quanta*. 1924, Migration-université en cours d'affectation.
19. Broglie, L.d., *XXXV. A tentative theory of light quanta*. The London, Edinburgh, and Dublin Philosophical Magazine and Journal of Science, 1924. **47**(278): p. 446-458.
20. Müller, H., A. Peters, and S. Chu, *A precision measurement of the gravitational redshift by the interference of matter waves*. Nature, 2010. **463**(7283): p. 926-929.
21. Wolf, P., et al., *Does an atom interferometer test the gravitational redshift at the Compton frequency?* Classical and Quantum Gravity, 2011. **28**(14): p. 145017.
22. Mueller, H., A. Peters, and S. Chu, *Reply to: atom gravimeters and the gravitational redshift*. arXiv preprint arXiv:1009.1838, 2010.
23. Sinha, S. and J. Samuel, *Atom interferometry and the gravitational redshift*. Classical and Quantum Gravity, 2011. **28**(14): p. 145018.

24. Einstein, A., *Ist die Trägheit eines Körpers von seinem Energieinhalt abhängig?* Annalen der Physik, 1905. **323**(13): p. 639-641.
25. Einstein, A., *The general theory of relativity*, in *The meaning of relativity*. 1922, Springer. p. 54-75.
26. Weinberg, S. and R.V. Wagoner, *Gravitation and cosmology: principles and applications of the general theory of relativity*. 1973, American Institute of Physics.
27. Landau, L.D. and E.M. Lifshitz, *Fluid Mechanics: Volume 6*. Vol. 6. 1987: Elsevier.
28. Eringen, A.C., *Mechanics of continua*. Huntington, 1980.
29. Newton, I., *Philosophiae naturalis principia mathematica*. Vol. 1. 1833: G. Brookman.
30. Carroll, S.M., *An introduction to general relativity: spacetime and geometry.* Addison Wesley, 2004. **101**: p. 102.
31. Arfken, G.B., H.J. Weber, and F.E. Harris, *Mathematical methods for physicists: a comprehensive guide*. 2011: Academic press.
32. Landau, L.D., et al., *Theory of elasticity*. Vol. 7. 1986: Butterworth-Heinemann Oxford.
33. Gibbons, G.W., *The maximum tension principle in general relativity.* Foundations of Physics, 2002. **32**(12): p. 1891-1901.
34. Schiller, C., *General relativity and cosmology derived from principle of maximum power or force.* International Journal of Theoretical Physics, 2005. **44**(9): p. 1629-1647.
35. Barrow, J.D. and G.W. Gibbons, *Maximum tension: with and without a cosmological constant.* Monthly Notices of the Royal Astronomical Society, 2015. **446**(4): p. 3874-3877.
36. Landau, L.D., E.M. Lifshitz, and E.M. Lifshits, *The Classical Theory of Fields: Volume 2*. Vol. 2. 1975: Butterworth-Heinemann.
37. Ogden, R.W., *Non-linear elastic deformations*. 1997: Courier Corporation.
38. AH, G., *Nonlinear Solid Mechanics: A Continuum Approach for Engineering*. 2000, Wiley.
39. Schwarzschild, K., *Über das gravitationsfeld eines massenpunktes nach der einsteinschen theorie*. Sitzungsberichte der königlich preussischen Akademie der Wissenschaften, 1916: p. 189-196.
40. Synge, J.L., *Relativity: the general theory.* 1960.
41. Perlick, V., *Ray optics, Fermat's principle, and applications to general relativity*. 2003: Springer Science & Business Media.
42. Einstein, A., *Uber einen die erzeugung und verwandlung des lichtes betreffenden heuristischen gesichtspunkt.* Collected Papers of Albert Einstein, 1989. **2**: p. 150-166.
43. Einstein, A., *Zur elektrodynamik bewegter körper*, in *Das Relativitätsprinzip: Eine Sammlung von Abhandlungen*. 1905, Springer. p. 26-50.
44. Griffiths, D.J. and D.F. Schroeter, *Introduction to quantum mechanics*. 2018: Cambridge university press.
45. Greiner, W., *Relativistic quantum mechanics*. Vol. 3. 1990: Springer.

46. Klein, O., *Quantentheorie und fünfdimensionale Relativitätstheorie*. Zeitschrift für Physik, 1926. **37**(12): p. 895-906.
47. Schiff, L., *Quantum mechanics 3rd edition (NewYork: McGraw-Hill)*. 1968.
48. Compton, A.H., *A quantum theory of the scattering of X-rays by light elements*. Physical review, 1923. **21**(5): p. 483.
49. Planck, M., *Über irreversible strahlungsvorgänge*, in *Von Kirchhoff bis Planck: Theorie der Wärmestrahlung in historisch-kritischer Darstellung*. 1897, Springer. p. 166-171.
50. Kiefer, C., *Quantum gravity*, in *Springer Handbook of Spacetime*. 2014, Springer. p. 709-722.
51. Rovelli, C., *Quantum gravity, Cambridge, UK: Univ*. 2004, Pr.
52. Misner, C., *Thorne K and Wheeler JA/Gravitation*. 1973, Freeman.
53. Birrell, N. and P. Davies, *Quantum Fields in Curved Space, Cambridge University Press, Cambridge, UK*. 1982.
54. Parker, L. and D. Toms, *Quantum field theory in curved spacetime*. Vol. 8. 2009: Cambridge university press Cambridge.
55. Suárez, A. and P.-H. Chavanis, *Hydrodynamic representation of the Klein-Gordon-Einstein equations in the weak field limit: General formalism and perturbations analysis*. Physical Review D, 2015. **92**(2): p. 023510.
56. Will, C.M., *Theory and experiment in gravitational physics*. Vol. 198. 1953: cambridge university press Cambridge.
57. Touboul, P., et al., *MICROSCOPE mission: Final results of the test of the equivalence principle*. Physical review letters, 2022. **129**(12): p. 121102.
58. Wald, R.M., *General relativity*. 2010: University of Chicago press.
59. Scientific, L. and K.C. Virgo, *Tests of general relativity with GWTC-3*. (No Title), 2021.
60. Regge, T. and J.A. Wheeler, *Stability of a Schwarzschild singularity*. Physical Review, 1957. **108**(4): p. 1063.
61. Zerilli, F.J., *Effective potential for even-parity Regge-Wheeler gravitational perturbation equations*. Physical Review Letters, 1970. **24**(13): p. 737.